Annals of Botany **132**: 655–670, 2023
https://doi.org/10.1093/aob/mcad114, available online at www.academic.oup.com/aob

ANNALS OF BOTANY
Founded 1887

PART OF A SPECIAL ISSUE ON CAM AT THE CROSSROADS

CAM photosynthesis in *Bulnesia retama* (Zygophyllaceae), a non-succulent desert shrub from South America

Daniel Mok[1], Arthur Leung[1], Peter Searles[2], Tammy L. Sage[1] and Rowan F. Sage[1,*]

[1]Department of Ecology and Evolutionary Biology, University of Toronto, 25 Wilcocks Street, Toronto, Ontario M5R3C6, Canada and [2]Centro Regional de Investigaciones Científicas y Transferencia Tecnológica de La Rioja (CRILAR-CONICET), Entre Ríos y Mendoza s/n, Anillaco (5301), La Rioja, Argentina
[*]For correspondence. E-mail r.sage@utoronto.ca

Received: 9 May 2023 Returned for revision: 19 July 2023 Editorial decision: 26 July 2023 Accepted: 23 August 2023

• **Background and Aims** *Bulnesia retama* is a drought-deciduous, xerophytic shrub from arid landscapes of South America. In a survey of carbon isotope ratios ($\delta^{13}C$) in specimens from the field, *B. retama* exhibited less negative values, indicative of CAM or C_4 photosynthesis. Here, we investigate whether *B. retama* is a C_4 or CAM plant.
• **Methods** Gas-exchange responses to intercellular CO_2, diurnal gas-exchange profiles, $\delta^{13}C$ and dawn vs. afternoon titratable acidity were measured on leaves and stems of watered and droughted *B. retama* plants. Leaf and stem cross-sections were imaged to determine whether the tissues exhibited succulent CAM or C_4 Kranz anatomy.
• **Key Results** Field-collected stems and fruits of *B. retama* exhibited $\delta^{13}C$ between −16 and −19 ‰. Plants grown in a glasshouse from field-collected seeds had leaf $\delta^{13}C$ values near −31 ‰ and stem $\delta^{13}C$ values near −28 ‰. The CO_2 response of photosynthesis showed that leaves and stems used C_3 photosynthesis during the day, while curvature in the nocturnal response of net CO_2 assimilation rate (A) in all stems, coupled with slightly positive rates of A at night, indicated modest CAM function. C_4 photosynthesis was absent. Succulence was absent in all tissues, although stems exhibited tight packing of the cortical chlorenchyma in a CAM-like manner. Tissue titratable acidity increased at night in droughted stems.
• **Conclusions:** *Bulnesia retama* is a weak to modest C_3 + CAM plant. This is the first report of CAM in the Zygophyllaceae and the first showing that non-succulent, xerophytic shrubs use CAM. CAM alone in *B. retama* was too limited to explain less negative $\delta^{13}C$ in field-collected plants, but combined with effects of low stomatal and mesophyll conductance it could raise $\delta^{13}C$ to observed values between −16 and −19 ‰. Modest CAM activity, particularly during severe drought, could enable *B. retama* to persist in arid habitats of South America.

Key words: *Bulnesia retama*, CAM photosynthesis, carbon isotope ratio, retamo, stem photosynthesis, xerophyte, Zygophyllaceae.

INTRODUCTION

The identification of species with photosynthetic carbon-concentrating mechanisms remains an ongoing task decades after the discovery of C_4 and crassulacean acid metabolism (CAM) photosynthesis (Frohlich *et al.*, 2022; Gilman *et al.*, 2023). Surveys of carbon isotope ratios ($\delta^{13}C$) using live plants or herbarium specimens readily identify C_3 and C_4 species, allowing C_4 clades to be mapped onto their respective phylogenies (Sage *et al.*, 2007; Lauterbach *et al.*, 2016, 2019). C_3 plants typically show $\delta^{13}C$ values between −21 and −32 ‰, whereas C_4 plants show values between −10 and −16 ‰ (Vogel, 1993; Cerling *et al.*, 1997; Sage *et al.*, 2007). A few species in lineages containing both C_3 and C_4 plants exhibit $\delta^{13}C$ values between −21 and −16 ‰ and are termed C_4-like species because they are evolutionary intermediates that operate a C_4 photosynthetic pathway but with incomplete enzyme compartmentalization (for example, *Flaveria brownii*, Monson *et al.*, 1988; and *Alloteropsis semialata*, Lundgren *et al.*, 2019). The other group of terrestrial plants with less negative $\delta^{13}C$ values typical of C_4 or C_4-like plants are CAM plants, which assimilate CO_2 at night via PEP carboxylase (PEPC) and use Rubisco to refix it during the day when stomata are closed (Kluge and Ting, 1978; Winter and Smith, 1996*a*; Winter and Holtum, 2002). Obligate CAM plants often exhibit a similar range of $\delta^{13}C$ values as C_4 plants, because most of the carbon in the plants enters at night via PEP carboxylation, during phase I of the CAM cycle (Osmond, 1978; Winter and Holtum, 2002; Edwards, 2019). Alternatively, many CAM species exhibit $\delta^{13}C$ values that overlap with typical C_3 values, and some exhibit $\delta^{13}C$ values of −16 to −20 ‰ that fall between the range of C_3 and C_4 values (Silvera *et al.*, 2010; Winter *et al.*, 2015; Messerschmid *et al.*, 2021). These species show intermediate contributions of PEP carboxylation to the overall pool of carbon in the plant, indicating co-function of a C_3 mode of photosynthesis and a CAM mode. The PEP carboxylation step discriminates less against $^{13}CO_2$ than does Rubisco carboxylation; hence, as the PEPC contribution to the carbon pool in a plant increases, its $\delta^{13}C$ value become less

negative (Farquhar and Lloyd, 1993). Based on empirical relationships between $\delta^{13}C$ and the fraction of daily carbon fixed at night by PEPC, Winter and Holtum (2002) predicted that plants having $\delta^{13}C$ values less negative than −20 ‰ acquire >50 % of their photosynthate via CAM. The term 'strong CAM' refers to these plants (Edwards, 2019; Hancock *et al.*, 2019; Sage *et al.*, 2023). Strong CAM plants also have pronounced CAM anatomical traits, notably high leaf succulence, whereby chloroplast-containing cells (chlorenchyma) have large vacuoles, tight cell packing and low intercellular air space (Nelson and Sage, 2008; Borland *et al.*, 2018; Edwards, 2019; Luján *et al.*, 2022). Weak CAM plants are largely C_3 in function, with low levels of succulence and low CAM activity (<5 % of daily C is acquired by CAM; Winter, 2019). Plants classified as C_3 + CAM obtain 5–50 % of their C from nocturnal CO_2 assimilation by PEPC and generally exhibit low to intermediate levels of succulence (Edwards, 2019; Winter, 2019; Luján *et al.*, 2022).

To identify species using C_4 or CAM photosynthesis, researchers in our laboratory, in collaboration with others, have been surveying $\delta^{13}C$ values in plant families common to arid and semi-arid landscapes (for example, Boraginaceae, Frohlich *et al.*, 2022; Nyctaginaceae, Khoshravesh *et al.*, 2020). In recent years, we have surveyed the photosynthetic pathway in the Zygophyllaceae, where two distinct C_4 lineages are identified, one in *Tetreana simplex* (= *Zygophyllum simplex* of the Zygophylloideae subgenus; Lauterbach *et al.*, 2016) and the other in the Tribuloideae subfamily (*Kallstroemia*, *Tribulus* and *Tribulopsis*; Lauterbach *et al.*, 2019). Results of our $\delta^{13}C$ survey for subfamilies Larreoideae, Seetzenioideae and Morkillioideae of the Zygophyllaceae are presented here for the first time.

In this survey, we observed mostly C_3-like $\delta^{13}C$ values; however, leaf and stem samples from herbarium specimens of one Larreoideae species, *Bulnesia retama* (Gillies ex Hook. & Arn.) Griseb., consistently showed C_4-like $\delta^{13}C$ values between −16 and −19 ‰. Ecological studies also noted $\delta^{13}C$ values between −17 and −24 ‰ in *B. retama* (Gatica *et al.*, 2017). *Bulnesia retama* (common name retamo) is a xerophytic drought-deciduous shrub from dry areas of Argentina and Peru (Fig. 1A; Ribas-Fernández *et al.*, 2009; Biruk *et al.*, 2022). It forms green stems and is common if not dominant across its geographical range and produces a flush of small compound leaves during the summer rainy season (Crisci *et al.*, 1979; Godoy-Bürki *et al.*, 2018; Biruk *et al.*, 2022). The leaves are deciduous, senescing at the end of the rainy season to yield an aphyllous stem canopy that persists throughout the dry season and is the source of retamo polishing and ink wax (Warth, 1956; Debandi *et al.*, 2002). This habit represents an interesting variation in the function of xerophytic shrubs, in that it allows for relatively high rates of photosynthesis in the moist season, while continuing carbon assimilation into the dry season using water use-efficient stems (Nilsen, 1995; Smith *et al.*, 1997). Smith *et al.* (1997) describe drought-deciduous shrubs (and trees) with green stems as being functionally intermediate between drought-evading deciduous shrubs and drought-resisting evergreen shrubs. They also note that deciduous xerophytic shrubs are largely C_3 unless they exhibit succulence, in which case they may be CAM.

The best-known species in the Larreoideae is the xerophytic evergreen shrub *Larrea tridentata* (creosote bush), an often-dominant C_3 plant from the warm deserts across southwestern North America (Rundel and Sharifi, 1993). It is recognized as having some of the lowest water potentials measured in any drought-tolerant species and is considered a flagship species of the Mojave, Chihuahuan and Sonoran deserts (Smith *et al.*, 1997; Supplementary Data Table S1). In South America, *B. retama* occupies many of the same habitats that *L. tridentata* does in North America, and it often co-occurs with other *Larrea* species, notably, the Southern Hemisphere counterpart to the creosote bush, termed *Larrea divaricata* (common name, jarillo or chaparral).

Less negative $\delta^{13}C$ values, approaching −21 ‰, are often observed in C_3 plants from dry climates (Ehleringer and Cooper, 1988; Ehleringer *et al.*, 1998; Sage *et al.*, 2007; Frohlich *et al.*, 2022). In the Larreiodeae, Gatica *et al.* (2017) observed $\delta^{13}C$ values in xerophytic *Larrea* and *Prosopis* shrubs in the *B. retama* habitat between −21 and −27 ‰. In *L. tridentata*, large variation in $\delta^{13}C$ can occur, from −32 ‰ in wet soil to −21 ‰ in very dry conditions (Rundel and Sharifi, 1993). In C_3 plants, the increase in $\delta^{13}C$ values is largely attributable to high diffusive resistance between the atmosphere and the chloroplast stroma caused by low stomatal (g_s) and mesophyll conductance (g_m, the diffusive conductance between the intercellular air space and the chloroplast interior) relative to net CO_2 assimilation rate (Farquhar *et al.*, 1989; Seibt *et al.*, 2008). Lower diffusive conductance relative to CO_2 assimilation rate allows for proportionally more ^{13}C to be fixed by Rubisco relative to ^{12}C, increasing $\delta^{13}C$ in leaf and stem tissue (Farquhar *et al.*, 1989; Seibt *et al.*, 2008). However, low conductance is rarely known to produce $\delta^{13}C$ values less negative than −20 ‰ in C_3 plants, and thus, such values commonly indicate the operation of a carbon-concentrating mechanism (Monson *et al.*, 1988; Cerling *et al.*, 1997; Winter and Holtum, 2002). For plants such as *B. retama*, $\delta^{13}C$ values between −16 and −19 ‰ are strong indicators that either C_4-like or CAM-like photosynthesis is a major source of carbon in the plant.

There are currently no experimental data evaluating the photosynthetic pathway of *B. retama* and no known instance of CAM within the Zygophyllaceae (Winter and Smith, 1996*b*; Gilman *et al.*, 2023). In this study, we first present $\delta^{13}C$ values from a survey of the Larreoideae, Morkillioideae and Seetzenioideae, then examine whether *B. retama* uses the C_4 or CAM photosynthetic pathway by assessing leaf and stem gas exchange, leaf and stem anatomy, and dawn vs. dusk acid titrations of leaves and stems.

MATERIALS AND METHODS

Growth conditions

We grew six *B. retama* plants in 20 L pots filled with a sandy loam in the glasshouse at the University of Toronto. Plants grew from seed collected in April 2015 at a xeric site in La Rioja, Argentina (28°48′S, 66°56′W; elevation 1325 m; 150 mm annual rainfall) dominated mostly by xerophytic shrubs (*B. retama*, *Larrea cuneifolia*, *Parkinsonia praecox* and *Senna aphylla*) with interspersed *Prosopis* trees. The shrubs in the glasshouse were trimmed to remain ~1 m tall. Beginning in the spring of 2023, we also grew six *Bulnesia foliosa* plants from seed that was collected from plants in an abandoned

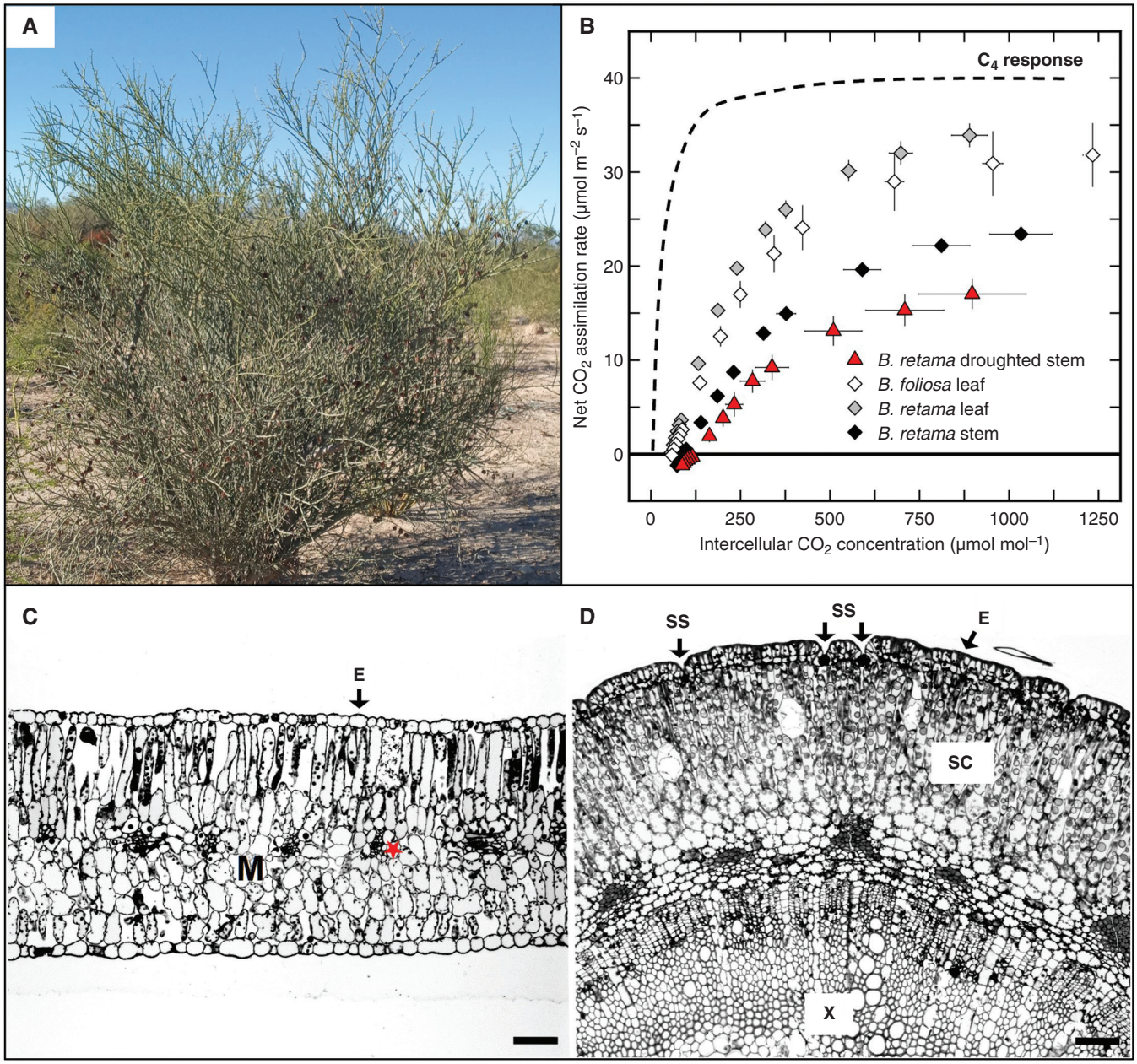

FIG. 1. (A) A photograph of *Bulnesia retama* in its native habitat in La Rioja, northwestern Argentina, showing mostly leafless green stems (photograph by Peter Searles). (B) The net CO_2 assimilation rate (A) vs. intercellular CO_2 concentration (C_i) of well-watered *Bulnesia foliosa* leaves (white diamonds; C_3), well-watered *B. retama* leaves and stems (grey and black diamonds, respectively) and moderately droughted *B. retama* stems (red triangles). Values are means ± s.e.m. Moderately droughted stems had a Ψ_w of −2.5 ± 0.1 MPa. Droughted leaves are not shown because *B. retama* is aphyllous under drought. The dashed line represents a well-watered C_4 A/C_i response from *Tribulus cistoides*. (C, D) Cross-sections of a *B. retama* leaf (C) and stem (D). Scale bars: 50 μm. Abbreviations: E, epidermis; M, mesophyll; red asterisk, bundle sheath cell; SC, stem cortex; SS, sunken stomata; X, secondary xylem.

roadside lot in La Rioja, Argentina; these plants were grown in 5 L pots of sandy loam. During the study period between July 2022 and July 2023, all plants were maintained in a glasshouse or plant growth chamber at approximately 30 °C day–25 °C night temperatures and with photosynthetic photon flux densities (PPFD) reaching 1600 μmol photons m^{-2} s^{-1} on sunny days (in the glasshouse), or 800 μmol m^{-2} s^{-1} at the top of the plant canopy (in the growth chamber). High-pressure sodium lamps in the glasshouse supplemented daily light intensities to maintain a constant photoperiod of 13 h over the year and a minimum PPFD of 250 μmol m^{-2} s^{-1} on cloudy days. Plants were fertilized weekly with a 50:50 mix of two commercial fertilizers (Plant-Products 21-7-7 Acid and 20-20-20 Classic; www.plantprod.com) supplemented with calcium nitrate and magnesium sulfate at Hoagland solution concentrations (Epstein, 1972). Three *B. retama* plants were drought treated and three served as well-watered controls.

Drought treatment and water potential measurements

The study consisted of two drought trials. In the first, pre-drought measurements started on 1 August and drought treatments began on 30 September 2022, using plants from the glasshouse. The water potential (Ψ_w) of stems with leaves (well-watered controls) or without leaves (drought treatments) was measured with a PMS model 600 pressure chamber (www.PMSinstruments.com) immediately before the start of the experimental dawn at 07:00 h. Experimental dawn was controlled by removing opaque tents over individual plants in the glasshouse at night, or by switching on lamps to begin the diurnal light cycle if plants were in growth chambers or the gas-exchange laboratory. The rate of pressure increase was approximately 0.5 MPa min^{-1}, which avoided overshoot of the end point. The drought treatment initially consisted of withholding water for 2 weeks, during which shoot Ψ_w declined to −5.5 to −6 MPa. Gas exchange and titratable acidity were determined after 14 days of no water, when plants had a mean Ψ_w at dawn of −5.7 MPa. Because the plants exhibited drought injury (darkening and wilting of stems) and had minimal gas exchange at this time, we designated the measurements as the 'extreme' drought set and instituted a limited water regime of 500 mL applied to each pot every other day, with a 500 mL fertilizer solution added weekly. On the 21st day after initiation of the drought treatment (20 October 2022), we reassessed gas exchange and titratable acidity, when plants had a mean Ψ_w of −3.8 MPa. This was designated our 'severe' drought stress. Thereafter, the limited watering regime stabilized the plant Ψ_w between −2 and −3 MPa, and the plants appeared healthy in terms of having visibly turgid, green stems. This became our 'moderate' drought treatment and was designated as the principal drought stress for the duration of the study. Gas exchange and titratable acidity were re-measured on glasshouse-grown plants on 3 or 4 November 2022. Given that gas-exchange rates declined with the arrival of the short, cloudy days of winter, we moved the plants to a Biochamber GC-20 growth chamber (www.Biochambers.com) in January 2023 and repeated the diurnal measurements after the plants had acclimated to the growth chamber and exhibited net CO_2 assimilation rates (A) similar to those observed in the glasshouse during the summer of 2022. The control and moderate drought-treated plants were maintained in the growth chamber. Growth chamber daylength was 13 h day–11 h night, with 30 °C days and 25 °C nights. After 14 days of acclimation in the chamber and full recovery of A, gas-exchange and titratable acidity measurements were repeated until the experiment ended on 2 March 2023, at which point all plants were fully rewatered and returned to the glasshouse.

The second drought trial began on 1 June 2023, by initiating a 15-day diurnal gas-exchange measurement on stems of two *B. retama* plants that were previously part of the non-droughted treatment. For the first 2 days, 1.5 L of water was supplied to maintain high Ψ_w. For the next 5 days (days 3–7), daily water was reduced in 250 mL increments per day from 1.5 L to 250 mL, which allowed pre-dawn Ψ_w of the plants to drop below −4 MPa by day 7. On day 7, daily water was increased to between 500 and 750 mL to bring Ψ_w to between −2 and −3 MPa until the end of the trial. After the 15-day diurnal measurements, we measured a 48-h diurnal response of stem gas exchange on droughted and well-watered stems of *B. retama* at 25 °C day–20 °C night to determine whether CAM increased in cooler temperatures. We also measured the CO_2 assimilation rate (A), net intercellular CO_2 partial pressure (C_i) and diurnal gas-exchange responses of non-droughted *B. foliosa* plants. Given that no C_4 or CAM activity was evident, *B. foliosa* served as our C_3 comparison.

Gas exchange

Gas-exchange measurements were conducted on leaves and stems using a LI-6400XT system with a 6 cm^2 leaf chamber (LI-COR Biosciences, Lincoln, NE, USA; www.licor.com). About 1.5 cm^2 of recent, fully expanded leaves, or two to three stems of 2 cm length were measured, with measured stem regions being two to three nodes below the shoot apex. Leaves were removed when measuring stem photosynthesis, and stems were excluded from the gas-exchange chamber during leaf measurements. All daytime gas-exchange measurements were conducted at light saturation (1000 μmol m^{-2} s^{-1}). Before and during drought, the response of net CO_2 assimilation rate (A) to variation in intercellular CO_2 partial pressure (C_i) was measured as described by Adachi *et al.* (2023). The diurnal response of gas exchange was measured at 400 μmol CO_2 mol^{-1} air and 30 °C over a 13-h day period and 25 °C over an 11-h night period. Measurements began at noon and continued for 24 h in trial 1, and for 15 days in drought trial 2. To simulate dusk during drought trial 1, we decreased PPFD by 200 μmol m^{-2} s^{-1} and temperature by 1 °C every 30 min in a ramp down to darkness. At the simulated dawn, temperature and light were increased at the same rate. In trial 2, the end-of-day ramp to darkness was changed to a 200 μmol m^{-2} s^{-1} and 1 °C decrease every 15 min, and the rate of ramp to full illumination in the morning was changed to a 200 μmol m^{-2} s^{-1} and 1 °C increase every 15 min. Leaf and stem area used for gas exchange were digitally imaged, with the projected area in two dimensions being determined using ImageJ image analysis software (Schneider *et al.*, 2012; https://imagej.net/).

Titratable acidity

We sampled ~1.5 cm^2 of leaf or 2 cm stem segments at 16:00 h (when tissue acidity was minimal) and at the experimental dawn (07:00 h, when tissue acidity would be at its peak) for determination of titratable acidity (Heyduk *et al.*, 2019). Tissue sampling followed criteria used for selecting gas-exchange samples. After sampling, the tissue was frozen in liquid N_2 and stored at −80 °C until assay. Immediately upon removal from the freezer and before tissue could thaw, we weighed the samples for fresh weight. Samples were then placed in 60 mL of 20 % EtOH, boiled to half volume, returned to 60 mL with dH_2O, boiled to half volume again, then returned to 60 mL with dH_2O again and allowed to cool to room temperature. Once cooled, we titrated the solution to pH 7.0 using 2 mM NaOH and calculated titratable acidity as follows:

$$\mu \text{ mol of } H^+ \text{per gram fresh weight} = \frac{\text{mL titrant} \times \left(2\ \mu \text{ mol mL}^{-1}\right)}{\text{Fresh weight (g)}}$$

Anatomy

Recently matured leaf and stem tissue was sampled for light microscopy between 08:00 and 10:00 h. Tissue was fixed in a 2 % glutaraldehyde solution in 0.2 M sodium cacodylate buffer (pH 7.4) and post-fixed in a 2 % osmium tetroxide solution. Samples were then dehydrated in 10 % EtOH increments and embedded in Araldite 502 resin (https://www.emsdiasum.com/). Embedded tissues were sectioned at 3 µm, stained with Toluidine Blue (O'Brien and McCully, 1981), and imaged using a Zeiss Axioplan microscope (https://www.zeiss.com/) with an image analysis system (model DP71, Olympus: EMPIX Imaging). The planar cross-sectional cell area of stem cortical or leaf mesophyll cells was quantified, as was the percentage of intercellular air space (% IAS) of leaf mesophyll or stem cortical tissue. For cross-sectional cell area, ten cells per leaf were measured randomly from palisade and spongy mesophyll from four leaves of each of four plants and from ten cortex cells of six stems from each of six plants. The % IAS was estimated using a point intercept method (Parkhurst, 1982). Images were analysed using a Cintiq graphics tablet (https://www.wacom.com/) and ImageJ software (Schneider *et al.*, 2012; https://imagej.net/).

$\delta^{13}C$ assays

For $\delta^{13}C$ assays, herbarium specimens of the Larreoideae were sampled at Kew Gardens or the Missouri Botanical Gardens (for voucher specimens and raw $\delta^{13}C$ values, see Supplementary Data Table S2). We also sampled live tissue from our plants grown in the glasshouse in Toronto and fruits with seeds of the source material collected in La Rioja, Argentina. Typically, $\delta^{13}C$ values were assayed on 0.5–2 mg leaf or stem tissue using mass spectroscopy at the University of California, Davis stable isotope facility (before 2015, Stable Isotope Facility (ucdavis.edu)) or the Washington State University stable isotope facility (after 2014; https://labs.wsu.edu/isotopecore/). None of the species assayed for $\delta^{13}C$ other than *B. retama* and *B. foliosa* was grown for physiological and anatomical analyses.

RESULTS

$\delta^{13}C$ survey

The $\delta^{13}C$ values for 70 specimens of 30 Larreoideae, Morkillioideae and Seetzenioideae species showed that all but one of the species exhibited C_3-like mean $\delta^{13}C$ values (Table 1; Supplementary Data Table S2). The exception is *B. retama*, for which herbarium specimens (largely stems) from five distinct *B. retama* collections and from the fruits and seeds from plants collected near La Rioja, Argentina, had $\delta^{13}C$ values between −16.1 and −18.9 ‰ (mean ± s.e.m. of −17.4 ± 0.4 ‰). All other *Bulnesia* species had $\delta^{13}C$ values ranging between −23.0 and −27.3 ‰. Notably, *B. retama* leaf and stem samples produced in the glasshouse in Toronto had C_3-like $\delta^{13}C$ values between −27 and −31.5 ‰ (Table 1), in contrast to the material collected in the native habitat, including the seeds from which these plants were grown. Of the non-*Bulnesia* species, two from the Larreoideae, *Pintoa chilensis* and *Porlieria arida*, had mean $\delta^{13}C$ values of −22.3 and −22.5 ‰, respectively, which are at the least negative end of the C_3 range.

Leaf and stem anatomy

Bulnesia retama leaves and stems lack anatomical traits associated with C_4 or strong CAM photosynthesis (Fig. 1C, D; Table 2). Ground tissue of the dorsiventral leaves was composed of elongate adaxial and abaxial palisade chlorenchyma, with the abaxial cells being shorter and wider. Numerous chlorenchyma cells were between bundle sheath cells, which lacked prominence in cross-section, with each bundle sheath cell having chloroplasts along its outer periphery as occurs in C_3 species (Fig. 1C; Dengler and Nelson, 1999; Stata *et al.*, 2014, 2016). Cylindrical stems of *B. retama* were composed of an epidermis with a thick waxy cuticle and sunken stomata, a cortex of chlorenchyma cells, and secondary xylem and phloem (Fig. 1D). Leaf mesophyll and stem cortex cells were not obviously succulent, being smaller than chlorenchyma cells of C_3 plants and well below the cross-sectional area of CAM chlorenchyma cells (Table 2; Nelson *et al.*, 2005). Stems exhibited a % IAS that was 7.5 % of the planar area of the cortex tissue in cross-section, below the mean % IAS of photosynthetic tissues in CAM plants (Fig. 1D; Table 2). In contrast, the % IAS of *B. retama* leaf mesophyll was similar to C_3 values in the study by Nelson *et al.* (2005; Table 2).

Gas-exchange measurements

Drought-treated *B. retama* plants lost all leaves 7–10 days after water cessation and relied completely on stem photosynthesis in the droughted state. Plants exhibited symptoms of severe drought stress at a Ψ_w near −4 MPa, such as darkening of stems and desiccation of stem tips, but appeared healthy, with green, turgid stems at a Ψ_w of −2 to −3 MPa, which we designated as our moderate drought treatment. Under moderate drought, *B. retama* did not grow new shoots.

Before and during the drought treatment, the responses of net CO_2 assimilation rate (A) vs. intercellular CO_2 (C_i) in leaves and stems of *B. retama* were assessed to determine whether any tissue conducted C_4 photosynthesis. No evidence of C_4 photosynthetic behaviour was detected, and all A/C_i responses were typical of C_3 photosynthesis (Fig. 1B). CO_2 compensation points (Γ) were 55 ± 1 µmol mol^{-1} (n = 5) in leaves and 90 ± 4 µmol mol^{-1} (n = 6) in stems, rather than near 0 µmol mol^{-1} as they would be if C_4 photosynthesis occurred. The A/C_i response of moderately droughted *B. retama* stems was also C_3-like (Γ = 126 ± 16 µmol mol^{-1}, n = 3), although A was reduced by the stress (Fig. 1B). Stem Γ is likely to be high owing to a large respiratory signal from heterotrophic vascular tissue (Kocurek *et al.*, 2020). The initial slope of the A/C_i responses in *B. retama* stems and leaves was well below the initial slope of the C_4 plant *Tribulus cistoides*, as is typical for C_3 vs. C_4 photosynthesis (Sage and Pearcy, 2000). In common with A/C_i responses of C_3 plants, the A/C_i response of *B. retama* leaves and stems and *B. foliosa* leaves did not show saturation until high C_i values >600 µmol mol^{-1} (Fig. 1B).

In *B. retama* leaves, diurnal gas-exchange responses showed no net nocturnal CO_2 fixation; however, weak CAM activity

TABLE 1. *$\delta^{13}C$ values from species within Zygophyllaceae subfamilies Larreoideae, Seetzenioideae and Morkillioideae.*

Taxa	$\delta^{13}C$ (‰)	Taxa	$\delta^{13}C$ (‰)
Larreoideae			
***Porlieria* clade (6/6)**			
Porlieria		*Bulnesia retama*	
angustifolia	−24.3 ± 1.1, *n* = 2	Glasshouse-grown leaf	−31.4 ± 0.3, *n* = 10
arida	−22.5 ± 1.2, *n* = 2	Glasshouse-grown stem (pre-drought)	−28.0 ± 0.2, *n* = 5
chilensis	−27.3, *n* = 1	Glasshouse-grown stem (droughted)	−28.5, *n* = 1
hygrometra	−25.9 ± 1.8, *n* = 2	Glasshouse-grown stem (control plants, no drought)	−27.5, *n* = 1
lorentzii	−26.0 ± 0.6, *n* = 2		
microphylla	−28.0 ± 0.5, *n* = 2		
***Guaiacum* clade (1/5)**		*B. schickendanzii*	−23.0 ± 0.05, *n* = 2
Guaiacum coulteri	−27.7, *n* = 1	*Pintoa chilensis*	−22.3 ± 1.0, *n* = 2
***Plectrocarpa* clade (2/2)**		**Larrea clade (1/5)**	
Plectrocarpa		*Larrea nitida*	−24.6 ± 0.5, *n* = 2
rougesii	−23.6, *n* = 1		
tetracantha	−25.7, *n* = 1		
***Gonopterodendron* clade (3/4)**			
Gonopterodendron		Note: Gatica *et al.* (2017) show that *L. cuneifolia* and *L. divaricata* plants in the field have C_3-like $\delta^{13}C$ values between −22 and −27 ‰ over a year. *Larrea tridentata* show a C_3-like $\delta^{13}C$ of −21 to −31 ‰ (Philpottt and Troughton, 1974; Ehleringer and Cooper, 1988; Rundel and Sharifi, 1993).	
aboreum	−25.1 ± 0.7, *n* = 4		
carrapo	−27.6, *n* = 1		
sarmientoi	−25.5 ± 0.7, *n* = 3		
***Bulnesia* s.s. *Pintoa–Metharme* clade (5/6)**		**Seetzenioideae (2/2)**	
Bulnesia		*Seetzenia*	
chilensis	−23.3, *n* = 1	*lanata*	−27.2 ± 0.4, *n* = 2
foliosa field-collected fruit	−26.5 ± 0.4, *n* = 3	*orientalis*	−27.0 ± 0.1, *n* = 2
foliosa glasshouse-grown leaf	−30.5 ± 0.7, *n* = 3	**Morkillioideae (3/5)**	
foliosa glasshouse-grown stem	−30.2 ± 0.1, *n* = 2	*Morkillia mexicana*	−24.4, *n* = 1
retama from herbaria	−17.5 ± 0.7, *n* = 5	*Sericodes greggi*	−24.2, *n* = 1
retama fruit wing (field collected)	−17.3 ± 0.5, *n* = 3	*Viscainoa geniculata*	−24.4 ± 0.02, *n* = 2

Taxonomy follows Godoy-Bürki *et al.* (2018) and Tropicos (www.Tropicos.com). Numbers in parentheses following a clade name indicate the number of species sampled/present in the clade. In total, 23 of 35 species (66 %) in these three subfamilies are sampled. For sample source and voucher information, see Supplementary Data Table S2.

was indicated by a slight curvature in the nocturnal response of *A*, whereby *A* became less negative in the middle of the night (Fig. 2A; Winter and Holtum, 2015). Daytime *A* in *B. retama* leaves exceeded 12 μmol m^{-2} s^{-1} , with typical C_3-like C_i/C_a ratios between 0.7 and 0.8 (Fig. 2A–C; Table 3). These responses are similar to those observed in the C_3 species *B. foliosa*, except that its nocturnal *A* response was C_3-like, with little curvature (Fig. 2G–I).

In the well-watered state, *B. retama* stems from the first drought trial often showed slight positive *A* early in the dark period, which became negative towards the end of the night (Figs 2B and 3A). Other stems exhibited slightly negative values of *A* in the early to middle of the night, after which *A* drifted more negative as dawn approached (Fig. 4A). In moderately droughted stems, *A* peaked near 8 μmol m^{-2} s^{-1} during the daytime in plants of the first drought trial (Figs 3B and 4D; Table 3). At night, *A* in these stems was slightly positive (Fig. 3B) or near zero (Fig. 4D) in the early to the middle of the night, after which it drifted negative. In severely stressed stems (Ψ_w of −3.4 to −4.5 MPa), daytime *A* fell to near

TABLE 2. *The size of photosynthetic cells and relative intercellular air space in* Bulnesia retama.

Organ	Tissue region	Area per cell (μm²)	Relative IAS (%)
Leaf	Palisade	1311 ± 68[a]	26.0 ± 2.3[a]
	Spongy	1161 ± 79[a]	
Stem	Cortex	597 ± 31[b]	8.2 ± 0.6[b]

Mean cell size and relative IAS (±s.e.m.) from Nelson *et al.* (2005)

Organ	Tissue region	Area per cell (μm²)	Relative IAS (%)
CAM leaf (n = 18 species)	Mesophyll	3260 ± 550	14.8 ± 1.7
C_3 leaf (n = 6 species)	Mesophyll	840 ± 230	31.6 ± 4.9
C_4 leaf (n = 4 species)	Mesophyll	620 ± 150	28.7 ± 5.5

Cell size is estimated as cross-sectional area in leaf or stem. The percentage of intercellular air space (% IAS) is the percetnage area of the IAS in planar cross-sections divided by the corresponding area of leaf mesophyll or stem cortical tissue. Values are the mean ± s.e.m. Superscripted letters indicate statistically different groups at $P < 0.05$ via one-way ANOVA and a Tukey's post-hoc test. For comparison, leaf mesophyll cell area in cross-section and % IAS are shown for CAM, C_3 and C_4 values from Nelson *et al.* (2005).

0 μmol m^{-2} s^{-1}, whereas nocturnal A showed initial positive rates which became negative late in the night (Fig. 4G, H). During extreme stress (Ψ_w of −5.9 MPa), *B. retama* stems showed negative A and minimal g_s in both day and night; however, the night response of A was curved, rising to near 0 μmol m^{-2} s^{-1} at ~20.00 h, then declining after midnight (Fig. 4J, K).

In the 15-day diurnal response of drought trial 2, A peaked near 8 μmol m^{-2} s^{-1}, then declined following water restriction, with low rates (nil to 1.5 μmol m^{-2} s^{-1}) present during severe drought on days 5–7 and with rates between 1 and 4 μmol m^{-2} s^{-1} on days 9–11 during moderate drought (Fig. 5A; Supplementary Data Table S3). Despite variation in daytime A, stems exhibited curved nocturnal responses of A as observed in watered to droughted plants of trial 1, in that A values were slightly positive or, if negative, were near 0 μmol m^{-2} s^{-1} in the early to middle of the night, then declined late in the dark period (Fig. 5A). On some nights, particularly when A was positive, the negative drift in A as dawn approached appeared pronounced (days 11–15 in Fig. 5A).

CAM activity did not increase in *B. retama* stems in cooler temperatures of 25°C day and 20°C night temperature (Supplementary Data Fig. S1), as occurs in some CAM species (Lüttge, 2004).

We estimated the contribution of nocturnal CO_2 fixation to the daily carbon budget in *B. retama* stems, as described in the legend to Table 4, to provide a rough idea of CAM contributions to daily carbon gain (Table 4). In well-watered stems, 12–14 % of the daily carbon gain is estimated to result from nocturnal carbon acquisition, whereas in moderately droughted stems, 13–25 % of the daily carbon gain is estimated to be acquired by CAM at night. In the severe or extremely droughted stems, the gross carbon assimilation at night shows little change compared with moderately droughted stems, but with the large reduction in carbon gain during the day, the nocturnal contribution by CAM rises to an estimated 42–49 % of the daily carbon gain (Table 4).

In well-watered and moderately droughted stems of trials 1 and 2, pronounced declines in g_s began in the early to middle of the afternoon (Figs 2E, 3C, D, 4B, E and 5B). This decline was associated with a reduction in C_i/C_a values from >0.6 to ≤0.5 (Figs 2F, 3E, F, 4C, F and 5C; Table 3; Supplementary Data Table S3). For example, in moderately droughted *B. retama* stems grown in the glasshouse, the midday C_i/C_a of 0.67 declined to 0.42 at 18.00 h. The decline in C_i/C_a indicates greater stomatal limitation reduces A in the later afternoon.

Titratable acidity

Nocturnal acid accumulation (ΔH^+) in *B. retama* stems was modest in stems of well-watered plants [mean of 22.4 ± 10.6 μmol H^+ g^{-1} fresh weight (FW)] and increased to a mean of 98.6 ± 23.7 μmol H^+ g^{-1} FW during moderate drought (Fig. 6; Table 5). In severe to extreme drought, ΔH^+ in stems was not significant. Values of ΔH^+ became negative below a Ψ_w of −4 MPa (Fig. 6). Leaf ΔH^+ was insignificant in well-watered and moderately droughted plants, although there was near significance in the ΔH^+ of droughted leaves (P = 0.8), suggesting an increase in titratable acidity at night immediately before their senescence (Table 5).

DISCUSSION

Our results demonstrate that *B. retama* stems largely use C_3 photosynthesis during the day but exhibit a weak CAM cycle at night that is strengthened during drought. Leaves largely function in a C_3 mode but might have weak CAM as indicated by slight curvature in the nocturnal response of A (Winter and Holtum, 2015), with a near-significant enhancement of nocturnal acidity when droughted. Because the leaves senesce when droughted, any enhancement of leaf CAM as soils dry would probably be of little consequence to annual carbon gain. There is no evidence of C_4 photosynthesis in *B. retama*, because plants had high Γ values and relatively low initial slopes of the A/C_i response and showed no evidence of C_4 anatomy, such as enlarged, organelle-enriched bundle sheath cells (Dengler and Nelson, 1999; Voznesenskaya *et al.*, 2005; Sage *et al.*, 2013). Previously, $\delta^{13}C$ values between −17 and −24 ‰ were observed at the beginning and end of the growing season in stems of *B. retama* located in the Monte Desert of Argentina, suggesting a variable photosynthetic strategy over the growing season (Gatica *et al.*, 2017). We also found evidence of a variable strategy, because leaves and stems from well-watered plants grown in Toronto exhibited C_3 $\delta^{13}C$ values between −27.5 and −31.5 ‰, while the fruits produced by the parents of these plants in their Argentinian habitat had a $\delta^{13}C$ average of −17.4 ‰. Large shifts in $\delta^{13}C$ are documented in non-succulent, xerophytic C_3 shrubs grown in moist vs. dry conditions; for example, in *L. tridentata*, $\delta^{13}C$ values range between −32 and −21 ‰; however, it is rare for $\delta^{13}C$ to be less negative than −21 ‰ in C_3 species (Philpott and Troughton, 1974; Rundel and Sharifi, 1993; Ehleringer *et al.*, 1998; Gatica *et al.*, 2017). We therefore suspected facultative CAM in stems as a possible explanation

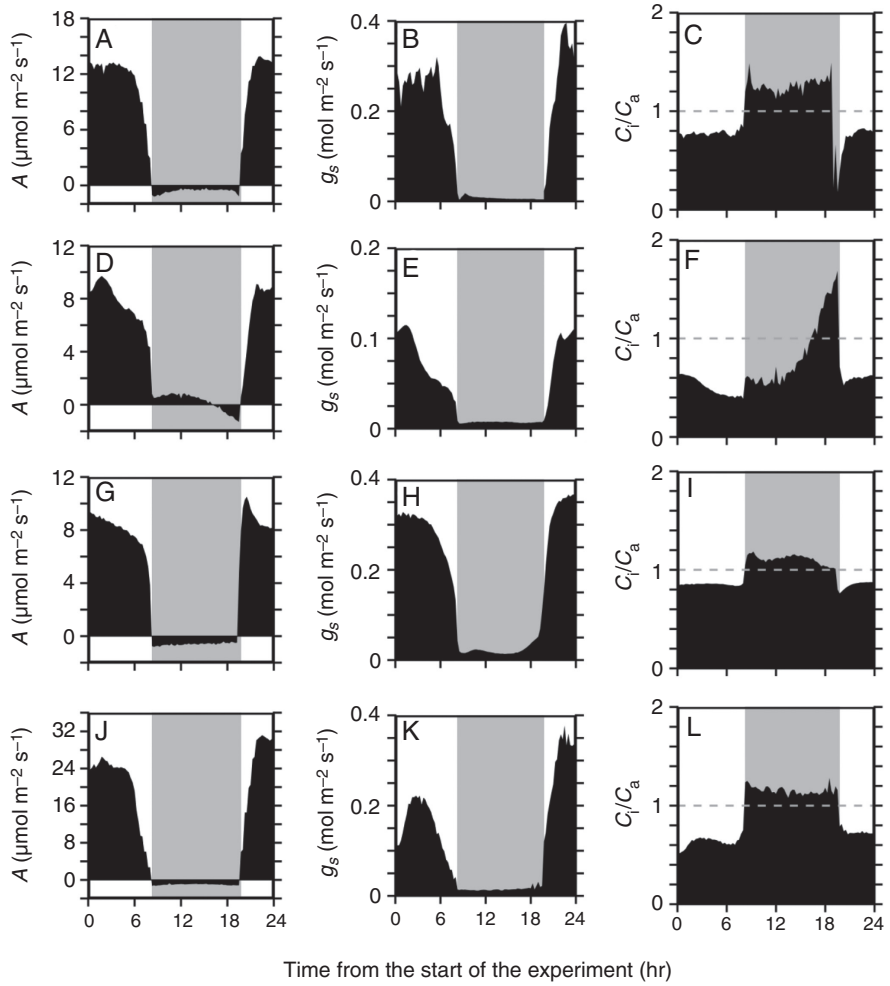

FIG. 2. Diurnal gas-exchange responses of well-watered *Bulnesia retama* leaves and stems, and from representative C_3 and C_4 species grown in the University of Toronto glasshouse facility. Plots show representative 13 h light and 11 h dark measurements of net CO_2 assimilation rate (*A*; A, D, G, J); stomatal conductance (g_s; B, E, H, K) and the ratio of intercellular to ambient CO_2 partial pressure (C_i/C_a; C, F, I, L) in a well-watered *B. retama* leaf (A–C) and stems (D–F), a well-watered *Bulnesia foliosa* leaf (C_3; G–I) and a well-watered *Tribulus cistoides* leaf (C_4; J–L). Experiments began at 12:00 h. Note dissimilar *y*-axes and positive nocturnal CO_2 assimilation rates in *B. retama* stems (panel D). The grey dashed line in the C_i/C_a plots indicates 1.0. Grey shading on each panel indicates the nocturnal period.

for the high $\delta^{13}C$ in field-grown *B. retama*. In the discussion below, we consider the evidence for CAM photosynthesis in *B. retama* along with other mechanisms that could explain its less negative $\delta^{13}C$ in the field.

We observed that net CO_2 assimilation rate (*A*) in *B. retama* stems is often positive early in the night, consistent with a weak CAM phase I. It drifted negative later during the dark period in a pattern observed in weaker C_3 + CAM species, such as those in *Calandrinia*, *Cistanthe*, *Pilea* and *Jatropha* (Winter and Holtum, 2015; Holtum *et al.*, 2017, 2021; Winter *et al.*, 2020). We also observed cases where *A* was slightly negative early in the night in *B. retama* stems, in which case the values of *A* also drifted more negative towards the end of the night. This is a pattern known as cryptic CAM and is observed in species such as *Jatropha curcas* and *Pilea peperomioides* (Winter and Holtum, 2015; Winter *et al.*, 2020). In *B. retama*, this pattern was typical in well-watered stems, indicating weak CAM activity. Our estimated gross CO_2 fixation contribution at night of 12–25 % in watered to moderately droughted plants (Table 4) qualifies *B. retama* as a weak to moderate C_3 + CAM species rather than a cryptic CAM species (Winter, 2019). Low nocturnal CO_2 fixation in *B. retama* stems could be explained, in part, by low tissue succulence of the cortical cells, which would not provide much volume for storing malate (Borland *et al.*, 2018). CAM plants with low storage potential tend to fill their vacuoles with organic acids earlier in the night, at which time the nocturnal rate of CO_2 fixation by PEP carboxylase begins to decline, and the estimated *A* value drops as stem respiration increasingly dominates the net flux of CO_2 (Winter and Holtum, 2015; Holtum *et al.*, 2017, 2021; Borland *et al.*, 2018). Such a decline was observed commonly in the nocturnal gas exchange of *B. retama*.

Titratable acidity in well-watered stems of *B. retama* is greater at dawn relative to late afternoon, with moderate drought increasing nocturnal acid accumulation (ΔH^+). In a survey of CAM in *Calandrinia*, well-watered plants exhibited $\Delta H^+ < 20$ μmol H^+ g^{-1} FW, slightly below the mean ΔH^+ of 22 μmol H^+ g^{-1} FW we observed in well-watered *B. retama*

TABLE 3. *Maximum day and night values of net CO_2 assimilation rate (A) in* Bulnesia retama*, with the corresponding stomatal conductance (g_s) and C_i/C_a plus late afternoon (18:00) values of* A*, g_s and C_i/C_a.*

Plant	Maximum values						Values 6 h after start of experiment (18:00 h)		
	Day			Night					
	A (μmol m^{-2} s^{-1})	g_s (mol m^{-2} s^{-1})	C_i/C_a	***A*** (μmol m^{-2} s^{-1})	g_s (mol m^{-2} s^{-1})	C_i/C_a	***A*** (μmol m^{-2} s^{-1})	g_s (mol m^{-2} s^{-1})	C_i/C_a
From Fig. 2 (glasshouse)									
Bulnesia retama leaf (Fig. 2A–C)	13.92	0.38	0.82	–0.26	0.06	1.15	11.84	0.25	0.77
Bulnesia retama stem (Fig. 2D–F)	9.71	0.11	0.61	0.87	0.08	0.52	6.84	0.05	0.42
Bulnesia foliosa leaf (C_3) Fig. 2G–I)	10.51	0.37	0.88	–0.41	0.04	1.18	7.61	0.26	0.84
Tribulus cistoides (C_4) (Fig. 2J–L)	31.18	0.28	0.41	–0.75	0.02	1.10	19.23	0.14	0.34
From Fig. 3 (growth chamber)									
Well-watered *B. retama* stem (Fig. 3A, C, E)	8.04 ± 2.33	0.11 ± 0.02	0.65 ± 0.31	0.42 ± 2.32	0.01 ± 0.02	0.77 ± 0.32	7.43 ± 0.52	0.07 ± 0.02	0.52 ± 0.05
Moderate drought *B. retama* stem (Fig. 3B, D, F)	8.21 ± 2.07	0.09 ± 0.02	0.58 ± 0.45	0.60 ± 1.99	0.01 ± 0.02	0.71 ± 0.45	8.04 ± 0.56	0.08 ± 0.02	0.56 ± 0.002
From Fig. 4 (glasshouse)									
Well-watered *B. retama* stem (Fig. 4A–C)	7.83	0.10	0.67	–0.14	0.003	1.18	4.19	0.04	0.52
Moderate drought *B. retama* stem (Fig. 4D–F)	8.97	0.13	0.67	–0.13	0.001	0.34	5.83	0.04	0.40
Severe drought *B. retama* stem (Fig. 4G–I)	0.50	0.01	0.71	0.68	0.002	–	0.22	0.01	0.80
Severe drought *B. retama* stem (Fig. 4J–L)	–0.01	0.01	0.97	–0.09	0.004	1.06	–0.33	0.004	1.33

Values are from the 24 h gas-exchange measurements presented in Figs 2–4. The Fig. 3 values are means ± s.e.m.

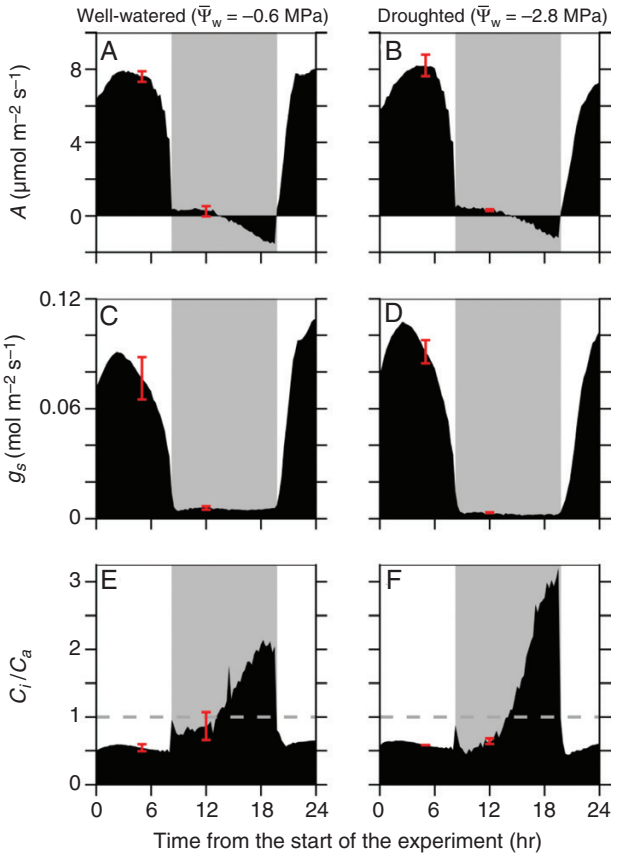

FIG. 3. Diurnal gas-exchange response of well-watered and moderately droughted *Bulnesia retama* stems grown in a plant growth chamber at the University of Toronto growth facility. The plots show mean net CO_2 assimilation rate (*A*; A, B), stomatal conductance (g_s; C, D) and the ratio of intercellular to ambient CO_2 partial pressure (C_i/C_a; E, F) during a 13 h light–11 h dark diurnal cycle for well-watered (A, C, E) and moderately droughted (B, D, F) *B. retama* stems from a growth chamber. Experiments began at 12:00 h. Mean Ψ_w value of well-watered plants is −0.6 ± 0.03 MPa and for droughted plants −2.8 ± 0.3 MPa (n = 3). Red bars indicate representative s.e.m. values. The grey dashed line in the C_i/C_a panels indicates 1.0. Grey shading in each panel indicates the nocturnal period.

stems. In droughted leaves of *Calandrinia volubulis*, ΔH^+ rose to a mean of 82 μmol H^+ g^{-1} FW, leading to its designation as a facultative CAM plant (Table 5; Hancock *et al.*, 2019). By this criterion, droughted *B. retama* stems would approximate facultative CAM behaviour, given that their mean ΔH^+ was 99 μmol H^+ g^{-1} FW. This shift in ΔH^+ was often associated either with less negative values of *A* at night or with the appearance of positive values of *A* during the early to mid-nocturnal period, in droughted relative to well-watered stems of *B. retama*. Consistently, when integrated over the dark period, the net C flux was less negative in moderately droughted compared with well-watered *B. retama* stems and became positive in the severely droughted stems during trial 1 (Table 4). Owing to variable dark respiration estimates, we could not detect consistent patterns in the gross CO_2 assimilation rate at night. By assuming that the stem respiration rate measured immediately before dawn was constant throughout the diurnal cycle, we estimated that dark CO_2 fixation contributed 13–25 % of the daily carbon gain (Table 4), leading us to consider *B. retama* a moderate C_3 + CAM plant when its CAM potential is induced fully. Consistent with a moderate CAM designation, the relative CAM contribution increased to near 50 % in severely droughted plants; however, this was attributable to large reductions in daytime *A*, rather than a strengthening of CAM activity.

The results presented here are the first to document CAM in *Bulnesia*, the Larreoideae, the Zygophyllaceae and the order Zygophyllales. This discovery raises the number of CAM plant families to 38 in 17 orders of terrestrial plants (Gilman *et al.*, 2023). We suspect that CAM is more widespread in the Zygophyllaceae, because several species have $\delta^{13}C$ values less negative than −23 ‰. We observed that the Larreoideae species *Pintoa chilensis* had a mean $\delta^{13}C$ of −22.3 ‰ and that in *Porlieria arida* it was −22.5 ‰. The Zygophylloideae, in particular, have numerous species with $\delta^{13}C$ values less negative than −21 ‰ (in addition to the C_4 plants in the *Tetraena simplex* complex). Lauterbach *et al.* (2016) lists five specimens from the Zygophylloideae with $\delta^{13}C$ values between −19 and −21 ‰, and one specimen of *Tetraena bucharica* was −18.8 ‰, which falls outside of the general C_3 range. The Tribuloideae species *Sisyndite spartea* also exhibits a $\delta^{13}C$ near −21 ‰ (Lauterbach *et al.*, 2019). Although Zygophyllaceae species represent some of the most extreme xerophytes known, with leathery to fleshy leaves, tolerance of low water potentials and repeated reliance on stem photosynthesis (Smith *et al.*, 1997; Gibson, 1996; Porter, 2016; Godoy-Bürki *et al.*, 2018), the only definitive evidence for CAM in the family is from *B. retama*. We encourage wider investigation before ruling out weak CAM or C_3 + CAM in other species of the family.

Possible mechanisms for less negative $\delta^{13}C$ in B. retama

The $\delta^{13}C$ values of −30 to −32 ‰ observed in *B. retama* and *B. foliosa* plants grown in the Toronto glasshouse reflect a 2–3 ‰ more negative $\delta^{13}C$ CO_2 source in the urban Toronto air relative to mid-20th century non-urban atmospheres (Graven *et al.*, 2020), coupled with strong C_3 contributions over the lifetime of the plant, when they were generally well watered and leafy. In the field, where there is no urban source of CO_2, hypothetical *B. retama* plants without CAM and sufficiently watered could be expected to exhibit $\delta^{13}C$ values near −27 ‰, as indicated by the mean $\delta^{13}C$ of −26.5 ‰ of field-collected *B. foliosa* fruits. Winter and Holtum (2002) used −27 ‰ as their pure C_3 reference value in modelling the response of $\delta^{13}C$ to increasing CAM strength. Based on their model, for a C_3 + CAM plant to exhibit $\delta^{13}C$ values near −17 ‰, 60 % of the daily CO_2 uptake must happen at night (Winter and Holtum, 2002; Hancock *et al.*, 2019; Winter, 2019). Hence, the level of CAM in well-watered to moderately droughted *B. retama* stems is insufficient to explain $\delta^{13}C$ values observed in field-collected material. Instead, the model described by Winter and Holtum (2002) predicts that the 13–25 % nocturnal C contribution estimated here for well-watered to moderately droughted stems of *B. retama* would increase $\delta^{13}C$ by ~1–4 ‰ units, to stem values of −26 to −23 ‰, assuming that $\delta^{13}C$ is −27 ‰ in purely C_3 *B. retama* (Winter and Holtum, 2002). The values of approximately −28 ‰ observed in stems of glasshouse-grown *B. retama* in Toronto are consistent with a 2–3 ‰ unit increase attributable to CAM, assuming non-CAM values of −30 to −31 ‰ occur in the functionally C_3 leaves of *B. retama* and *B. foliosa*.

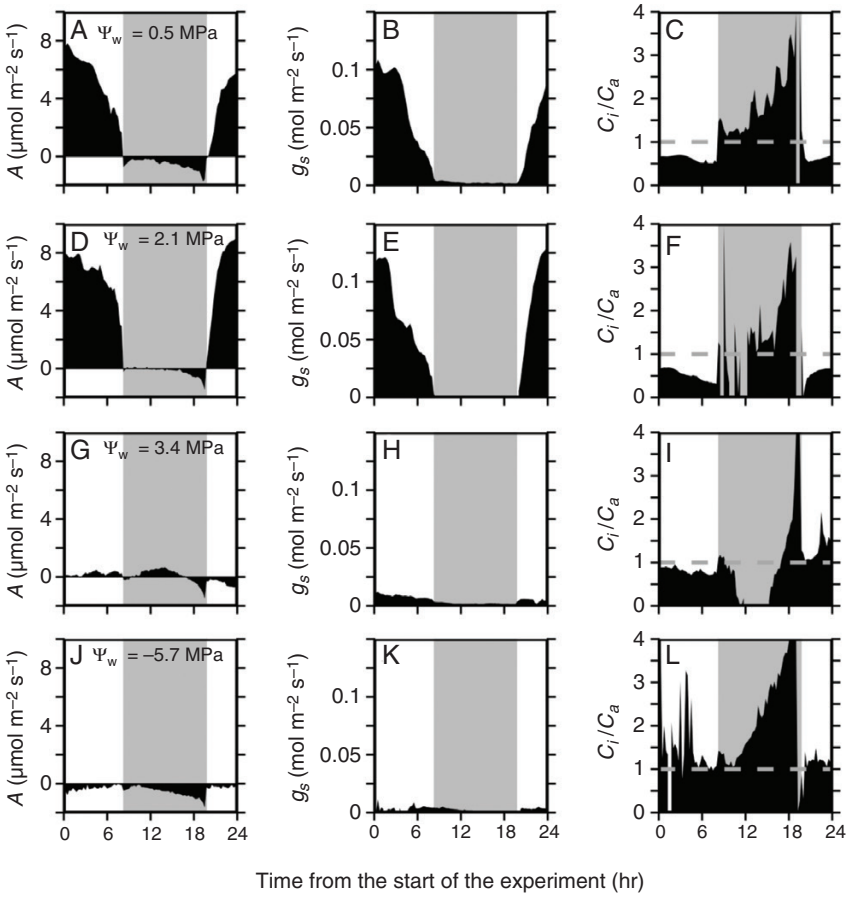

FIG. 4. Diurnal gas-exchange responses of glasshouse-grown *Bulnesia retama* stems experiencing varying degrees of drought. Plots show responses over a 13 h light–11 h dark period in well-watered and droughted *B. retama* stems from glasshouse-grown plants. The responses shown are net CO_2 assimilation rate (*A*; A, D, G, J), stomatal conductance (g_s; B, E, H, K) and the ratio of intercellular to ambient partial pressure of CO_2 (C_i/C_a; C, F, I, L) in stems of glasshouse-grown *B. retama* plants. (A–C) Responses of well-watered plants. (D–F) Responses of moderately droughted stems. (G–I) Responses of severely droughted plants. (J–L) Responses during extreme drought. Experiments began at 12:00 h. Each response is from one representative plant. The grey dashed line in the C_i/C_a plots indicates 1.0. Grey shading in each panel indicates the nocturnal period.

One possible cause of less negative $\delta^{13}C$ in field *B. retama* samples is that the plants exist in a severely droughted state for enough of the year that the CAM contribution dominates the annual carbon budget. In severely droughted *B. retama* stems, we estimated that the CAM contribution rose to 49 % of the daily C uptake. This increase in the CAM contribution was not attributable to increased CAM activity in an absolute sense, but rather, from a large drop in the C_3 contribution during the day. Although severe drought over a lengthy dry season could increase the CAM contribution to the annual carbon budget, we do not anticipate that the increase would approach values required to explain field $\delta^{13}C$ values in *B. retama*. In their native habitat of the Monte desert, Argentina, the growing season of *B. retama* ranges from October to March, when summer rains occur and minimal to moderate drought can be expected (Gatica *et al.*, 2017). This length, coupled with the much higher daytime rates of carbon gain relative to nocturnal CAM activity that would occur on moist to moderately dry soils, does not indicate that CAM would dominate the yearly carbon budget. We therefore hypothesize that a mechanism other than CAM contributes to the less negative $\delta^{13}C$ values in *B. retama* plants from the field. With C_4 photosynthesis unlikely, this mechanism is probably low diffusive conductance in *B. retama* stems.

To evaluate diffusion limitations in stems, we modelled the relationship between $\delta^{13}C$ and stem C_i/C_a (the ratio of intercellular CO_2 concentration to atmospheric CO_2 concentration) using eqn (10) in the paper by Cernusak *et al.* (2013):

$$\delta^{13}C = -7.5 - \left[a + (b - a)\left(\frac{C_i}{C_a}\right)\right] \quad (1)$$

where *a* is diffusional fractionation and *b* is carboxylation fractionation by Rubisco. The term *a* is typically 4.4 ‰, *b* is 27 ‰, and the source air around the time when the herbarium specimens of *B. retama* were collected would have been near −7.5 ‰. The C_i/C_a ratio reflects the balance between leaf or stem conductance and *A*; as it increases, $\delta^{13}C$ declines in a linear relationship in C_3 plants (Farquhar *et al.*, 1989). Equation 1 is a simplified relationship that incorporates effects of mesophyll diffusion limitations into the *b* term, which is commonly taken as 27 ‰ when carbon isotopic discrimination is modelled as a function of term C_i/C_a for a typical C_3 leaf (Cernusak *et al.*, 2013). At a typical C_i/C_a for C_3 leaves of 0.75 and $b = 27$ ‰,

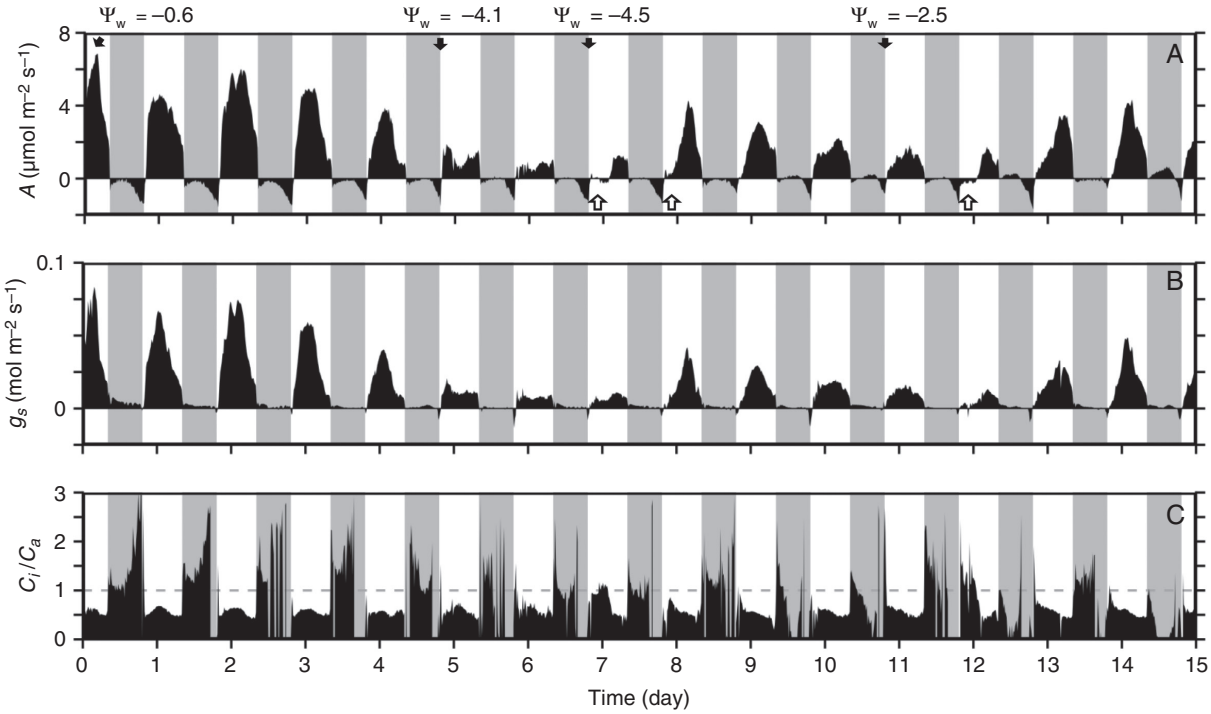

FIG. 5. Diurnal gas-exchange responses of *Bulnesia retama* stems over a 15-day period, during which severe and then moderate drought treatments were imposed on initially well-watered plants. Diurnal net CO_2 assimilation rate (A), stomatal conductance (g_s) and the ratio of intercellular to ambient CO_2 partial pressure (C_i/C_a) over a 15-day period of controlled water stress with 13 h light–11 h dark photoperiod from one representative glasshouse-grown *B. retama* plant in drought trial 2. The experiment began at 12:00 h on day 0. The plant was given water each day at 10:00 h; 1.5 L of water on the first 2 days, decreasing to 250 mL over 5 days in 250 mL increments on each day until day 7, and 500–750 mL thereafter. White arrows indicate days when the plants received an additional 250 mL above the regular 500 mL of water owing to low photosynthetic rates indicative of drought stress. Black arrows represent plant Ψ_w values measured at 07:00 h, which are indicated in megapascals. The grey dashed line in the C_i/C_a panel indicates 1.0. See Supplementary Data Table S3 for summaries of gas-exchange values at 0:00, 10:00, 12:00, 14:00 and 18:00 h. Grey shading indicates the mocturnal periods.

TABLE 4. *Estimations of diurnal and nocturnal net and gross CO_2 assimilation in* Bulnesia retama *stems, and the proportion of gross CO_2 assimilation acquired at night.*

Condition	Net CO_2 assimilation					
	Integrated net CO_2 assimilation (mmol m^{-2} day^{-1})		Integrated gross CO_2 assimilation (mmol m^{-2} day^{-1})			
	Light period (13 h)	Dark period (11 h)	Light period (13 h)	Dark period (11 h)	%D	Estimated respiration rate (μmol m^{-2} s^{-1})
Growth chamber, Fig. 3						
Well watered	300 ± 18	−10 ± 11	371 ± 10	52 ± 15	12	−1.6 ± 0.3
Moderate drought	282 ± 31	−3 ± 3	344 ± 32	52 ± 4	13	−1.4 ± 0.04
Glasshouse, Fig. 4						
Well watered	213	−21	290	47	14	−1.7
Moderate drought	292	−7	358	52	13	−1.5
Severe drought	−0.3	6	67	65	49	−1.5
Extreme drought	−13	−22	61	44	42	−1.7
Glasshouse, Fig. 5						
Well watered, day 1	187	−17	245	39	14	−1.4
Moderate drought, day 10	58	−2	91	31	25	−0.8

Growth chamber values are means ± s.e.m. Glasshouse values are derived from individual plants. Daily CO_2 assimilation was calculated as the area under the curve from measurements of net CO_2 assimilation rate in Figs 3A, B, 4A, D, G, J and 5A. To estimate gross CO_2 assimilation, dark respiration rate was estimated at the end of the dark period and was assumed to be constant over day and night intervals. The respiration rate was then integrated over the 13 h day period and 11 h night periods and added to the day and night integrated CO_2 assimilation values. %D is the proportion of 24 h gross CO_2 assimilation acquired during the dark period and is calculated as: $[A_{dark}/(A_{dark} + A_{light})] \times 100\%$.

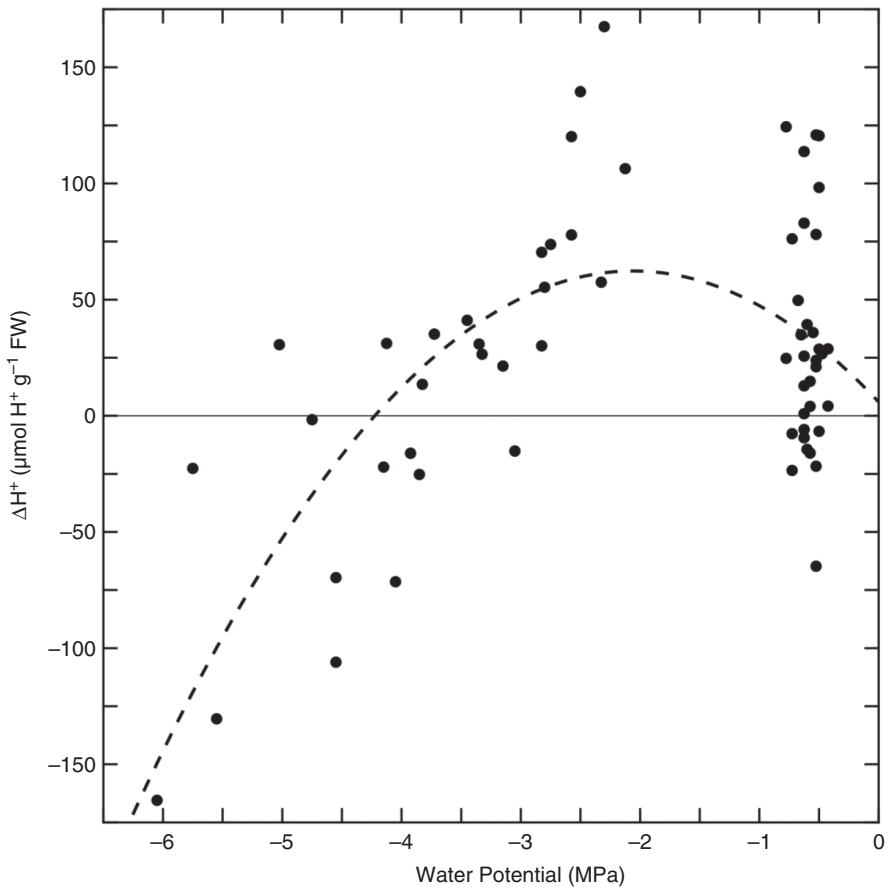

FIG. 6. The difference in titratable acidity (ΔH^+) of stem tissue sampled at 07:00 and 14:00 h vs. water potential at 07:00 h in *Bulnesia retama* stems. Each point is a single ΔH^+ for paired stems sampled on the same day. The dashed line represents a best-fitting polynomial regression ($y = -13.3\ x^2 - 54.8x + 5.9$; $R^2 = 0.41$, $P < 0.001$) for the slope value.

the predicted $\delta^{13}C$ is −28.9 ‰ (or −30.9 ‰, assuming that the $\delta^{13}C$ for Toronto source CO_2 is −9.5 ‰). Tight cell packing in cortical tissue and the associated low % IAS is a common feature in photosynthetic stems of xerophytes (Gibson, 1983, 1996; Nilsen, 1995), which reduces mesophyll conductance (Maxwell *et al.*, 1997) and, in turn, the value of *b* (Seibt *et al.*, 2008). Other features of *B. retama* that are common to xerophytes include sunken stomata, low stomatal density, thick waxy cuticles and small stomatal aperture (Biruk *et al.*, 2022). These xeromorphic features act in concert with low g_s to reduce stem conductance (Šantrůček, 2022), and are accounted for in eqn (1) as a lower C_i/C_a.

We observed daytime C_i/C_a in watered and moderately droughted *B. retama* stems to be between 0.67 and 0.4 (Table 3), which, using eqn (1), would correspond to modelled $\delta^{13}C$ of −27.0 to −20.9 ‰, respectively. If we assume that *b* is 26 ‰ to account for reduced mesophyll conductance from tight cell packing, the predicted range of $\delta^{13}C$ becomes −26.4 to −20.5 ‰. Our measurements, however, were conducted at vapour pressure deficits of 1–2 kPa, not at the values of >3 kPa common in the native habit of *B. retama* (Biruk, 2021). High vapour pressure deficit normally reduces g_s and C_i/C_a, with the integrated effect being a lower daily mean C_i/C_a because early-day maxima are reduced and afternoon declines begin earlier (Schulze and Hall, 1982; Cernusak *et al.*, 2019; Grossiod *et al.*, 2020). A mean field C_i/C_a of 0.4 would thus seem reasonable for *B. retama* stems, such that the modelled $\delta^{13}C$ of −20.5 ‰ is plausible. If we then add a 4 ‰ increase owing to modest nocturnal CAM activity, the stem $\delta^{13}C$ estimate is −16.5 ‰, which is consistent with the least negative $\delta^{13}C$ values observed in field-collected *B. retama* here and by Gatica *et al.* (2017).

The above exercise demonstrates how less negative $\delta^{13}C$ values in *B. retama* might be explained by a plausible combination of modest CAM and diffusion limitations. Follow-up research is needed to show how *B. retama* achieves its high $\delta^{13}C$ values, using real-time isotopic determinations (via starch or online discrimination measurements), accounting for effects of g_s, mesophyll conductance, drought and vapour pressure deficit in the *B. retama* habitat.

Conclusion: the role of CAM in B. retama

Although thousands of xerophytic plant species are known, it is a rarity to observe $\delta^{13}C$ values less negative than −20 ‰ in C_3 plants lacking CAM or C_4-like photosynthesis. Because of this, the $\delta^{13}C$ values of −16 to −19 ‰ observed in field-grown *B. retama* led us to hypothesize CAM or C_4 function. Modest C_3 + CAM function was observed, but this was too

TABLE 5. *Titratable acidity in* Bulnesia retama *plants at varying drought intensity.*

Organ	Water potential	Titratable acidity (μmol H^+ g^{-1} FW)			
	Ψ_w (MPa)	Afternoon	Dawn	ΔH^+	*P*-value
Measured values - leaf					
Well watered	−0.6 ± 0.01	89.1 ± 6.6	86.3 ± 6.1	−2.8 ± 8.9	$P = 0.62$
Moderate drought	−2.6 ± 0.1	91.3 ± 7.4	138.1 ± 15.0	46.9 ± 22.2	$P = 0.08$
Measured values - stem					
Well watered	−0.6 ± 0.01	114.6 ± 11.4	137.0 ± 21.8	22.4 ± 10.6	**$P = 0.046$**
Moderate drought	−2.4 ± 0.1	131.0 ± 20.9	229.7 ± 43.0	98.6 ± 23.7	**$P = 0.013$**
Severe drought	−3.5 ± 0.2	148.5 ± 21.4	159.2 ± 26.6	10.6 ± 12.2	*ns*
Extreme drought	−5.0 ± 0.3	224.2 ± 35.4	154.9 ± 21.3	−69.3 ± 41.3	*ns*
Literature values			Mean ± s.d.		
Agave americana	–	18.1 ± 4.6	331.1 ± 28.9	313	–
Calandrinia flava					
Watered	–	–	–	13.1 ± 2.0	–
Droughted	–	–	–	27.6 ± 2.2	–
Re-watered	–	–	–	24.3 ± 7.0	–
Calandrinia volubilis					
Watered	–	–	–	3.2 ± 1.9	–
Droughted	–	–	–	82.2 ± 11.6	–
Re-watered	–	–	–	23.8 ± 2.7	–

Titratable acidity of leaf or stem tissue was determined in the afternoon (16:00 h) and at dawn (07:00 h). Values are the mean ± s.e.m. ($n = 3$ plants per treatment). Differences between ΔH^+ means were tested using Student's one-tailed *t*-test, where all ΔH^+ values from a given plant were pooled to give one value per plant for the category of water status shown. For comparison, values from Winter and Smith (2022) for strong CAM *Agave americana* (Asparagaceae) and from Hancock *et al.* (2019) for C_3 + CAM *Calandrinia flava* and *C. volubilis* (Montiaceae) are shown. FW is fresh weight.

little to explain field $\delta^{13}C$ values unless we accounted for high diffusive limitations common in xerophytic shrubs, including *B. retama*. These results represent the first evidence of CAM in the non-succulent, xerophytic shrub functional type that is common to dominant across the arid and semi-arid zones of the Earth. Although some succulent, xerophytic shrubs use C_4 photosynthesis (mainly in the Amaranthaceae family or the Polygonaceae genus *Calligonum*; Sage and Pearcy, 2000), they are largely considered as being C_3, with a range of fitness strategies for xeric environments including thermodynamic drought tolerance, tight stomatal control, waxy cuticles with sunken stomata, drought deciduousness and photosynthetic stems (Gibson, 1996; Smith *et al.*, 1997). In *B. retama*, CAM photosynthesis can now be added to the mix of strategies conferring fitness in xeric environments in non-succulent, xerophytic shrubs. As with other weak to modest CAM plants (Griffiths, 1989; Holtum *et al.*, 2017), *B. retama* shrubs rely predominantly on C_3 photosynthesis in moist to moderately dry soils for the bulk of their carbon, but with the contributions of CAM, they are well poised to maintain a positive carbon balance and thus viability when extreme drought curtails C_3 carbon gain. As a result, CAM might allow them to occupy drier sites in the arid landscapes of South America, such as the Monte desert of Argentina, where they persist on extreme sandy soils and where their roots do not reach the water table (Ribas-Fernández *et al.*, 2009; Gatica *et al.*, 2017; Biruk, 2021; Biruk *et al.*, 2022).

We close with a reminder. Delineations of CAM often depend upon $\delta^{13}C$ surveys, with −20 ‰ commonly taken as the threshold between strong and modest CAM (Winter and Holtum, 2002). If low conductance produces $\delta^{13}C$ values approaching −21 ‰, weak to modest CAM could be interpreted erroneously as strong CAM. Such possibilities should be kept in mind when assessing CAM using $\delta^{13}C$ alone.

SUPPLEMENTARY DATA

Supplementary data are available at *Annals of Botany* online and consist of the following: Table S1: the *Larrea* pledge, which illustrates the significance of *Larrea tridentata* to ecologists in the American Southwest. Table S2: the source information and raw $\delta^{13}C$ values for 70 specimens of 30 species from the Larreoideae, Morkillioideae and Seetzenioideae subfamilies of the Zygophyllaceae. Table S3: gas-exchange values at key times during the 15-day diurnal trial shown in Fig. 5. Figure S1: 48-h response of *A* for well-watered and moderately droughted *B. retama* stems at 25 and 20 °C night.

FUNDING

This research was supported by NSERC Discovery grant RGPIN-2017-06476 to R.F.S., RGPIN-2020-05925 to T.L.S., and a Queen Elizabeth II/Charles E. Eckenwalder Scholarship in Science and Technology to A.L.

ACKNOWLEDGEMENTS

We thank Ria Patel for assistance with training D. Mok in microscopy methods. We also thank Bruce Hall, Bill Cole and Tom Gludovacz for taking care of the *B. retama* plants.

LITERATURE CITED

Adachi S, **Stata M**, **Martin DG**, ***et al***. **2023**. The evolution of C_4 photosynthesis in *Flaveria* (Asteraceae): insights from the *Flaveria linearis* complex. *Plant Physiology* **191**: 233–251. doi:10.1093/plphys/kiac467.

Biruk LN. 2021. *Ecofisiología de especies leñosas del Monte Central: aportes para la selección de especies y métodos de cultivo para la restauración de tierras secas*. Doctoral dissertation, University of Buenos Aires, Buenos Aires.

Biruk LN, **Fernández ME**, **González CV**, **Guevara A**, **Rovida-Kojima E**, **Giordano CV. 2022**. High and diverse plastic responses to water availability in four desert woody species of South America. *Trees* **36**: 1881–1894. doi:10.1007/s00468-022-02335-8.

Borland AM, **Leverett A**, **Hurtado-Castano N**, **Hu R**, **Yang X. 2018**. Functional anatomical traits of the photosynthetic organs of plants with crassulacean acid metabolism In: **Adams WW III**, **Terashima I**, eds. *Advances in photosynthesis and respiration, Vol. 44. The leaf: a platform for performing photosynthesis*. Berlin: Springer International, 281–305. doi:10.1007/978-3-319-93594-2_10

Cerling TE, **Harris JM**, **MacFadden BJ**, ***et al***. **1997**. Global vegetation change through the Miocene/Pliocene boundary. *Nature* **389**: 153–158. doi:10.1038/38229.

Cernusak LA, **Ubierna N**, **Winter K**, **Holtum JAM**, **Marshall JD**, **Farquhar GD. 2013**. Environmental and physiological determinants of carbon isotope discrimination in terrestrial plants. *New Phytologist* **200**: 950–965. doi:10.1111/nph.12423.

Cernusak LA, **Goldsmith GR**, **Arend M**, **Siegwolf RTW. 2019**. Effect of vapor pressure deficit on gas exchange in wild-type and abscisic acid-insensitive plants. *Plant Physiology* **181**: 1573–1586. doi:10.1104/pp.19.00436.

Crisci JV, **Hunziker JH**, **Palacios RA**, **Naranjo CA. 1979**. A numerical–taxonomic study of the genus *Bulnesia* (Zygophyllaceae): cluster analysis, ordination and simulation of evolutionary trees. *American Journal of Botany* **66**: 133–140. doi:10.1002/j.1537-2197.1979.tb06205.x.

Debandi G, **Rossi B**, **Aranibar J**, **Ambrosetti JA**, **Peralta IE. 2002**. Breeding system of *Bulnesia retama* (Gillies ex Hook & Arn.) Gris. (Zygophyllaceae) in the Central Monte Desert (Mendoza, Argentina). *Journal of Arid Environments* **51**: 141–152. doi:10.1006/jare.2001.0924.

Dengler NG, **Nelson T. 1999**. Leaf structure and development in C_4 plants In: **Sage RF**, **Monson RK**, eds. *C4 plant biology*. San Diego: Academic Press, 133–172. doi: 10.1016/B978-012614440-6/50006-9

Edwards EJ. 2019. Evolutionary trajectories, accessibility and other metaphors: the case of C_4 and CAM photosynthesis. *New Phytologist* **223**: 1742–1755. doi:10.1111/nph.15851.

Ehleringer JR, **Cooper TA. 1988**. Correlations between carbon isotope ratio and microhabitat in desert plants. *Oecologia* **76**: 562–566. doi:10.1007/BF00397870.

Ehleringer JR, **Rundel PW**, **Palma B**, **Mooney HA. 1998**. Carbon isotope ratios of Atacama desert plants reflect hyperaridity of region in Northern Chile. *Revista Chilena de Historia Natural* **71**: 79–86.

Epstein E. 1972. *Mineral Nutrition of plants: principles and perspectives*. New York: Wiley and Sons.

Farquhar GD, **Lloyd J. 1993**. Carbon and oxygen isotope effects in the exchange of carbon dioxide between terrestrial plants and the atmosphere In: **Ehleringer JR**, **Hall AE**, **Farquhar GD**, eds. *Stable isotopes and plant carbon-water relations*. San Diego: Academic Press, 47–70. doi:10.1016/B978-0-08-091801-3.50011-8.

Farquhar GD, **Ehleringer JR**, **Hubick KT. 1989**. Carbon isotope discrimination and photosynthesis. *Annual Review of Plant Physiology and Plant Molecular Biology* **40**: 503–537. doi:10.1146/annurev.pp.40.060189.002443.

Frohlich MW, **Sage RF**, **Craven LA**, ***et al***. **2022**. Molecular phylogenetics of *Euploca* (Boraginaceae): homoplasy in many characters, including the C_4 photosynthetic pathway. *Botanical Journal of the Linnean Society* **199**: 497–537. doi:10.1093/botlinnean/boab082.

Gatica MG, **Aranibar JN**, **Pucheta E. 2017**. Environmental and species-specific controls on $\delta^{13}C$ and $\delta^{15}N$ in dominant woody plants from central-western Argentinian drylands. *Austral Ecology* **42**: 533–543. doi:10.1111/aec.12473.

Gibson AC. 1983. Anatomy of photosynthetic old stems of nonsucculent dicotyledons from North American deserts. *Botanical Gazette* **144**: 347–362. doi:10.1086/337383. https://www.jstor.org/stable/2474431.

Gibson AC. 1996. *Structure-function relations of warm desert plants*. Berlin: Springer, 91–116. doi:10.1007/978-3-642-60979-4

Gilman IS, **Smith JAC**, **Holtum JAM**, **Sage RF**, **Winter K**, **Edwards EJ. 2023**. The CAM lineages of planet Earth. *Annals of Botany* (submitted, this volume).

Godoy-Bürki AC, **Acosta JM**, **Aagesen L. 2018**. Phylogenetic relationships within the New World subfamily Larreoideae (Zygophyllaceae) confirm polyphyly of the disjunct genus *Bulnesia*. *Systematics and Biodiversity* **16**: 453–468. doi:10.1080/14772000.2018.1451406.

Graven H, **Keeling RF**, **Rogelj J. 2020**. Changes to carbon isotopes in atmospheric CO_2 over the industrial era and into the future. *Global Biogeochemical Cycles* **34**: e2019GB006170. doi:10.1029/2019GB006170.

Griffiths H. 1989. Carbon dioxide concentrating mechanisms and the evolution of CAM in vascular epiphytes. In: **Lüttge U**, ed. *Vascular plants as epiphytes: evolution and ecophysiology*. Berlin: Springer-Verlag, 42–86.

Grossiod C, **Buckley TN**, **Cernusak LA**, ***et al***. **2020**. Plant responses to rising vapor pressure deficit. *New Phytologist* **226**: 1550–1566. doi:10.1111/nph.16485.

Hancock LP, **Holtum JAM**, **Edwards EJ. 2019**. The evolution of CAM photosynthesis in Australian *Calandrinia* reveals lability in C_3+CAM phenotypes and a possible constraint to the evolution of strong CAM. *Integrative and Comparative Biology* **59**: 517–534. doi:10.1093/icb/icz089.

Heyduk K, **Hwang M**, **Albert V**, ***et al***. **2019**. Altered gene regulatory networks are associated with the transition from C_3 to crassulacean acid metabolism in *Erycina* (Oncidiinae: Orchidaceae). *Frontiers in Plant Science* **9**: 1–15. doi:10.3389/fpls.2018.02000.

Holtum JAM, **Hancock LP**, **Edwards EJ**, **Winter K. 2017**. Facultative CAM photosynthesis (crassulacean acid metabolism) in four species of *Calandrinia*, ephemeral succulents of arid Australia. *Photosynthesis Research* **134**: 17–25. doi:10.1007/s11120-017-0359-x.

Holtum JAM, **Hancock LP**, **Edwards EJ**, **Winter K. 2021**. CAM photosynthesis in desert blooming *Cistanthe* of the Atacama, Chile. *Functional Plant Biology* **48**: 691–702. doi:10.1071/fp20305.

Khoshravesh R, **Stata M**, **Adachi S**, **Sage TL**, **Sage RF. 2020**. Evolutionary convergence of C_4 photosynthesis: a case study in the Nyctaginaceae. *Frontiers in Plant Science* **11**: 1–21. doi:10.3389/fpls.2020.578739.

Kluge M, **Ting IP. 1978**. *Crassulacean acid metabolism*. Berlin: Springer-Verlag. doi:10.1007/978-3-642-67038-1_5

Kocurek M, **Kornas A**, **Wierzchnicki R**, **Lüttge U**, **Miszalski Z. 2020**. Importance of stem photosynthesis in plant carbon allocation of *Clusia minor*. *Trees* **34**: 1009–1020. doi:10.1007/s00468-020-01977-w.

Lauterbach M, **van der Merwe PDW**, **Keßler L**, **Pirie MD**, **Bellstedt DU**, **Kadereit G. 2016**. Evolution of leaf anatomy in arid environments – a case study in southern African *Tetraena* and *Roepera* (Zygphyllaceae). *Molecular Phylogenetics and Evolution* **97**: 129–144. doi:10.1016/j.ympev.2016.01.002.

Lauterbach M, **Zimmer R**, **Alexa AC**, ***et al***. **2019**. Variation in leaf anatomical traits relates to the evolution of C_4 photosynthesis in Tribuloideae (Zygophyllaceae). *Perspectives in Plant Ecology, Evolution and Systematics* **39**: 125463. doi:10.1016/j.ppees.2019.125463.

Luján M, **Oleas NH**, **Winter K. 2022**. Evolutionary history of CAM photosynthesis in neotropical *Clusia*: insights from genomics, anatomy, physiology and climate. *Botanical Journal of the Linnean Society* **199**: 538–556. doi:10.1093/botlinnean/boab075.

Lundgren MR, **Dunning LT**, **Olofsson JK**, ***et al***. **2019**. C_4 anatomy can evolve via a single developmental change. *Ecology Letters* **22**: 302–312. doi:10.1111/ele.13191.

Lüttge U. 2004. Ecophysiology of crassulacean acid metabolism (CAM). *Annals of Botany* **93**: 629–652. doi:10.1093/aob/mch087.

Maxwell K, **von Caemmerer S**, **Evans JR. 1997**. Is a low internal conductance to CO_2 diffusion a consequence of succulence in plants with Crassulacean acid metabolism? *Australian Journal of Plant Physiology* **24**: 777–786. doi:10.1071/PP97088.

Messerschmid TFE, **Wehling J**, ***et al.* 2021**. Carbon isotope composition of plant photosynthetic tissues reflects a crassulacean acid metabolism (CAM) continuum in the majority of CAM lineages. *Perspectives in Plant Ecology, Evolution and Systematics* **51**: 125619. doi:10.1016/j.ppees.2021.125619.

Monson RK, **Teeri JA**, **Ku MSB**, **Gurevitch J**, **Mets LJ**, **Dudley S. 1988**. Carbon-isotope discrimination by leaves of *Flaveria* species exhibiting different amounts of C_3- and C_4-cycle co-function. *Planta* **174**: 145–151. doi:10.1007/BF00394765.

Nelson EA, **Sage RF. 2008**. Functional constraints of CAM leaf anatomy: tight cell packing is associated with increased CAM function across a gradient of CAM expression. *Journal of Experimental Botany* **59**: 1841–1850. doi:10.1093/jxb/erm346.

Nelson EA, **Sage TL**, **Sage RF. 2005**. Functional leaf anatomy of plants with crassulacean acid metabolism. *Functional Plant Biology* **32**: 409–419. doi:10.1071/FP04195.

Nilsen ET. 1995. Stem photosynthesis: extent, patterns, and role in plant carbon economy In: **Gartner BL**, ed. *Plant stems: physiology and functional morphology*. San Diego: Academic Press, 223–240. DOI: 10.1016/B978-012276460-8/50012-6

O'Brien TP, **McCully ME. 1981**. *The study of plant structure: principles and selected methods*. Melbourne: Termarcarphi. ISBN: 0959417400

Osmond CB. 1978. Crassulacean acid metabolism: a curiosity in context. *Annual Review of Plant Physiology* **29**: 379–414. doi:10.1146/annurev.pp.29.060178.002115.

Parkhurst DF. 1982. Stereological methods for measuring internal leaf structure variables. *American Journal of Botany* **69**: 31–39. doi:10.1002/j.1537-2197.1982.tb13233.x.

Philpott J, **Troughton JH. 1974**. Photosynthetic mechanisms and leaf anatomy of hot desert plants. *Carnegie Institute of Washington Yearbook* **73**: 790–793.

Porter DM. 2016. Zygophyllaceae R. Brown. In: Flora of North America Editorial Committee, eds. *Flora of North America*, Vol. **3**. Oxford: Oxford University Press, 28–42. ISBN: 9780190643720

Ribas-Fernández Y, **Quevedo-Robledo L**, **Pucheta E. 2009**. Pre- and post-dispersal seed loss and soil seed dynamics of the dominant *Bulnesia retama* (Zygophyllaceae) shrub in a sandy Monte desert of western Argentina. *Journal of Arid Environments* **73**: 14–21. doi:10.1016/j.jaridenv.2007.12.001.

Rundel PW, **Sharifi MR. 1993**. Carbon isotope discrimination and resource availability in the desert shrub *Larrea tridentata*. In: **Ehleringer JR**, **Hall AE**, **Farquhar GD**, eds. *Stable isotopes and plant carbon-water relations*. San Diego: Academic Press, 47–70. doi:10.1016/B978-0-08-091801-3.50019-2

Sage RF, **Pearcy RW. 2000**. The physiological ecology of C_4 photosynthesis In: **Leegood RC**, **Sharkey TD**, **von Caemmerer S**, eds. *Advances in photosynthesis and respiration. Photosynthesis: physiology and metabolism*. Dordrecht: Springer Netherlands, 497–532. doi:10.1007/0-306-48137-5_21

Sage RF, **Sage TL**, **Pearcy RW**, **Borsch T. 2007**. The taxonomic distribution of C_4 photosynthesis in Amaranthaceae sensu stricto. *American Journal of Botany* **94**: 1992–2003. doi:10.3732/ajb.94.12.1992.

Sage TL, **Busch FA**, **Johnson DC**, ***et al*. 2013**. Initial events during the evolution of C_4 photosynthesis in C_3 species of *Flaveria*. *Plant Physiology* **163**: 1266–1276. doi:10.1104/pp.113.221119.

Sage RF, **Gilman IS**, **Smith JAC**, **Edwards EJ**, **Silvera K. 2023**. Atmospheric CO_2 decline and the timing of CAM plant evolution. *Annals of Botany* (submitted this volume).

Šantrůček J. 2022. The why and how of sunken stomata: does the behaviour of encrypted stomata and the leaf cuticle matter? *Annals of Botany* **130**: 285–300. doi:10.1093/aob/mcac055.

Scheider CA, **Rasband WS**, **Eliceiri KW. 2012**. NIH image to ImageJ: 25 years of image analysis. *Nature Methods* **9**: 671–675. doi:10.1038/nmeth.2089.

Schulze E-D, **Hall AE. 1982**. Stomatal responses, water loss and CO_2 assimilation rates of plants in contrasting environments In: **Lange OL**, **Nobel PS**, **Osmond CB**, **Ziegler H**, eds. *Encyclopedia of plant physiology new series. Physiological plant ecology II: water relations and carbon assimilation*. Berlin: Springer-Verlag, 181–230. doi:10.1007/978-3-642-68150-9_8

Seibt U, **Rajabi A**, **Griffiths H**, **Berry J. 2008**. Carbon isotopes and water use efficiency: sense and sensitivity. *Oecologia* **155**: 441–454. doi:10.1007/s00442-007-0932-7.

Silvera K, **Neubig KM**, **Whitten WM**, **Williams NH**, **Winter K**, **Cushman J. 2010**. Evolution along the crassulacean acid metabolism continuum. *Functional Plant Biology* **37**: 995–1010. doi:10.1071/FP10084.

Smith SD, **Monson RK**, **Anderson JE. 1997**. *Physiological ecology of North American desert plants*. Berlin: Springer. doi:10.1007/978-3-642-59212-6

Stata M, **Sage TL**, **Rennie TD**, ***et al*. 2014**. Mesophyll cells of C_4 plants have fewer chloroplasts than those of closely related C_3 plants. *Plant, Cell & Environment* **37**: 2587–2600. doi:10.1111/pce.12331.

Stata M, **Sage TL**, **Hoffmann N**, **Covshoff S**, **Wong GKS**, **Sage RF. 2016**. Mesophyll chloroplast investment in C_3, C_4 and C_2 species of the genus *Flaveria*. *Plant and Cell Physiology* **57**: 904–918. doi:10.1093/pcp/pcw015.

Vogel JG. 1993. Variability of carbon isotope fractionation during photosynthesis. In **Ehleringer JR**, **Hall AE**, **Farquhar GD**, eds. *Stable isotopes and plant carbon-water relations*. San Diego: Academic Press, 29–46.

Voznesenskaya EV, **Koteyeva NK**, **Chuong SDX**, **Akhani H**, **Edwards GE**, **Franceschi VR. 2005**. Differentiation of cellular and biochemical features of the single-cell C_4 syndrome during leaf development in *Bienertia cycloptera* (Chenopodiaceae). *American Journal of Botany* **92**: 1784–1795. doi:10.3732/ajb.92.11.1784.

Warth AH. 1956. *The chemistry and technology of waxes*, 2nd edn. New York: Reinhold.

Winter K. 2019. Ecophysiology of constitutive and facultative CAM photosynthesis. *Journal of Experimental Botany* **70**: 6495–6508. doi:10.1093/jxb/erz002.

Winter K, **Holtum JAM. 2002**. How closely do the $\delta^{13}C$ values of crassulacean acid metabolism plants reflect the proportion of CO_2 fixed during day and night? *Plant Physiology* **129**: 1843–1851. doi:10.1104/pp.002915.

Winter K, **Holtum JAM. 2015**. Cryptic crassulacean acid metabolism (CAM) in *Jatropha curcas*. *Functional Plant Biology* **42**: 711–717. doi:10.1071/FP15021.

Winter K, **Smith JAC. 1996*a***. An introduction to crassulacean acid metabolism. Biochemical principles and ecological diversity In: **Klaus W**, **Smith JAC**, eds. *Crassulacean acid metabolism*. Berlin: Springer, 1–13. doi:10.1007/978-3-642-79060-7_1

Winter K, **Smith JAC. 1996*b***. Crassulacean acid metabolism: current status and perspectives In: **Klaus W**, **Smith JAC**, eds. *Ecological studies. Crassulacean acid metabolism: biochemistry, ecophysiology and evolution*. Berlin: Springer, 389–426. doi:10.1007/978-3-642-79060-7_26

Winter K, **Smith JAC. 2022**. CAM photosynthesis: the acid test. *New Phytologist* **233**: 599–609. doi:10.1111/nph.17790.

Winter K, **Holtum JAM**, **Smith JAC. 2015**. Crassulacean acid metabolism: a continuous or discrete trait? *New Phytologist* **208**: 73–78. doi:10.1111/nph.13446.

Winter K, **Garcia M**, **Virgo A**, **Smith JAC. 2020**. Low-level CAM photosynthesis in a succulent-leaved member of the Urticaceae, *Pilea peperomioides*. *Functional Plant Biology* **48**: 683–690. doi:10.1071/fp20151.